ISSN 0915-633X

NATIONAL INSTITUTE FOR FUSION SCIENCE

Laser-Driven Vehicles
- from Inner-Space to Outer-Space -

T. Yabe, C. Phipps, K. Aoki, M. Yamaguchi, Y. Ogata, M. Shiho, G. Inoue,
M. Onda, K. Horioka, I Kajiwara, S. Maehara and K. Yoshida

(Received - Apr. 24, 2002)

NIFS-735 June 2002

RESEARCH REPORT
NIFS Series

TOKI, JAPAN

Laser-Driven Vehicles - from Inner-Space to Outer-Space -

Takashi Yabe, Claude Phipps[a], Keiichi Aoki, Masashi Yamaguchi, Youichi Ogata,
Makoto Shiho[b], Gen Inoue[c], Masahiko Onda[d], Kazuhiko Horioka,
Itsuro Kajiwara, Sunao Maehara and Kunio Yoshida[e]

Tokyo Institute of Technology, Tokyo 152-8552, Japan
[a] *Photonic Associates, 200A Ojo de la Vaca Road, Santa Fe, NM 87505, USA*
[b] *Japan Atomic Energy Research Institute, Ibaragi 310-0193 Japan*
[c] *National Institute for Environmental Studies, Tsukuba, Ibaraki 305-8506 Japan*
[d] *National Institute of Advanced Industrial Science and Technology, Tsukuba, Ibaraki, 305-8564 Japan*
[e] *Osaka Institute of Technology, Osaka 535, Japan*

ABSTRACT

Laser supported propulsion of a micro-airplane with water-covered ablator is demonstrated. The repetitive use of overlay structure is experimentally demonstrated with specially-designed water supply. The various transparent overlay is investigated by the CIP-based hydrodynamic code and experiments by pendulum and semi-conductor load cell. The momentum coupling efficiency of 5000 N·sec/MJ has been achieved by ORION experiments that agree with the simulation code. With the maximum efficiency $\sim 10^5$ N·sec/MJ predicted by the simulation, 30 pulses of MJ laser can give the sound speed to 10 tons airplane. The concept can also be used for driving a micro-ship inside human body and a robot under the accidental circumstance of nuclear power reactor in which large amount of neutron source makes electronic device useless.

Keywords: Laser Propulsion, Airplane, Micro-ship, Human body, X-ray laser, Robot

1. INTRODUCTION

Kantrowitz proposed using laser ablation as an alternative to chemical propulsion for space vehicles in 1972.[1] The driving laser is located on the Earth, and no additional source of thrust is required on the vehicles. Recent developments in high power lasers show that this idea is realistic.[2–4] In fact, the vertical launch of a 100-g rocket has already been demonstrated.[3]

As an important near-future application, we propose a propulsion concept in which a laser drives a micro-airplane, and demonstrate it by experiments with a 590mJ/5ns YAG laser. The successful flight of the airplane relies on the enhanced coupling concept. For at least 30 years,[5] solid transparent overlays on absorbing surfaces have been used as a way of enhancing surface pressure and the laser momentum coupling coefficient due to pulsed lasers. The use of such concept for target acceleration appeared as an application to laser-driven fusion. The efficiency enhancement is attributed to the cannonball effect suggested by Winterberg,[6] Azechi[7] and Yabe[8] independently. The first two[6,7] used an enclosed configuration (like a real cannon) and the latter[8] employed a transparent overlay which was introduced to laser propulsion by Fabbro[9] and Phipps.[10] Although the enhancement is encouraging, the repetitive use of the structure is the key issue for realistic application. In this paper we shall propose a practical concept for laser-supported airplane and investigate the process in detail by experiments and simulations.

Adding to this, we propose several near-term applications of this concept. These are kite-plane, X-ray laser-driven micro-ship inside the human body, airship for telecommunication and so on. These subjects are now in consideration with joint project among (1) Tokyo Institute of Technology, (2) Photonic Associates, (3) Osaka Institute of Technology, (4) Japan Atomic Energy Research Institute (JAERI), (5) National Institute for Environmental Studies and (6) National Institute of Advanced Industrial Science and Technology in Japan.

In section 2, the coupling theories are reviewed and compared with each other. Section 3 provides experimental investigation of single- and multi-layered targets together with simulations. Demonstration of the micro-airplane is given in section 4 followed by water supply concept for repetitive impulse. Section 5 gives future applications of this concept.

2. ENHANCED COUPLING THEORY

Although Anderholm[5] observed enhanced coupling in overlay targets, he did not consider the acceleration ef-

ficiency but simply attributed the enhancement to reduced plasma production. In 1976, two different theories appeared on the quantitative estimation of the coupling efficiency. One is based on the concept of cannon ball. Winterberg[6] considered simple momentum conservation of two materials indicated by suffices 1 and 2.

$$M_1 U_1 = M_2 U_2. \tag{1}$$

where M is the total mass and U the velocity. Then kinetic energy gained by each target is

$$\frac{E_1}{E_2} = \frac{M_1 U_1^2}{M_2 U_2^2} = \frac{M_2}{M_1}. \tag{2}$$

Thus the most of the energy goes to lighter target ($E_1 \ll E_2$ for $M_1 \gg M_2$). In order to increase the efficiency, he proposed to place a heavier material as shown Fig.1.

This theory seems to be reasonable but we can not get rid of enhancement because large amount of ablated material is needed for high efficiency. That is, $E_1 = E_2$ is obtained only by $M_1 = M_2$ which means the ablated material must be the same as the target and we need to carry a large amount of "fuel" like a normal rocket. In contrast to this momentum theory, also in 1976 one of the authors Yabe[8] considered a situation in which metal target is covered with transparent and heavy material , and laser beam penetrates through the transparent layer and then deposits the energy at the interface. Yabe applied the blast wave theory to this situation in which two shock waves are generated in two materials after the energy is transmitted through the layer on the laser side and absorbed at the interface as shown in Fig.2. This analysis can be done by a self-similar solution but Yabe obtained the same conclusion as the exact solution by using simple estimation. Suppose the two shock waves driven in two directions and the momentum flow carried by these shock waves is

$$\rho_1 U_1^2 = \rho_2 U_2^2. \tag{3}$$

where ρ is the density. Thus the flow of kinetic energy W carried by each shock waves is

$$\frac{W_1}{W_2} = \frac{\rho_1 U_1^3}{\rho_2 U_2^3} = \left(\frac{\rho_2}{\rho_1}\right)^{1/2}. \tag{4}$$

Interestingly, this last relation is exactly the same as that for the total energy flow W carried by shock waves when the exact self similar solution is used.[11] Thus the efficiency is determined only from the density not from total mass. This conclusion is very important and instantaneous efficiency of coupling only depends on the ablation mass density. Actually as shown later on, high-efficiency acceleration has been achieved only with small ablator mass which is 1/10 of target.

3. PENDULUM EXPERIMENTS AND SIMULATIONS

First of all, we shall investigate the effect of ablator structure both by experiments and simulations. Two types of experiments have been done. One is the time-integrated measurement of momentum of target with pendulum and time-resolved measurement of exerting force by a load cell. Although the numerical simulation on these processes are very important to resolve them, the phenomena consist of complex processes like melting and evaporation together with large deformation of material interface, and thus the numerical scheme to solve solid, liquid and gas simultaneously is required to deal with drastic change of density. In this paper, we investigate laser propulsion by numerical simulation code PARCIPHAL based on the CIP-CUP method[12] that can satisfy such a demand, and evaluate effects caused by the difference of target structure like a multi-layered target that consists of metal layer over-coated with transparent material.

The simulation code PARCIPHAL includes absorption processes by conduction electron and plasmas, thermal conduction, viscosity, elastic-plastic deformation, hydrodynamics and equation of state considering latent heat. This code demonstrated its accuracy and ability in simulating laser cutting and ablation process in femto-second, nano-second, micro-second and milli-second laser pulses.[13]

The simulation of ablation processes is performed in axi-symmetric two- dimensional configuration. Incident laser beam is assumed to have the Gaussian shape both in time and space. Once the maximum laser intensity I_0, pulse duration τ, focusing radius r_0 are given as parameter , then the momentum coupling coefficient C_m[N·sec/MJ] is defined as the ratio of target momentum to incident laser pulse energy L during the ejection of laser-ablated material (the photoablation process).

$$C_m = \frac{m\triangle u}{L}, \quad L = I_0 \cdot \pi r_0^2 \tau \frac{\sqrt{\pi}}{2} \tag{5}$$

where $m\triangle u$ is the momentum of target obtained after laser irradiation. The exerting force is calculated by summing up the pressure along the target surface and integrating it in time.

In the followings, we shall investigate two types of target, standard target (hereafter ST) and exotic target(hereafter ET) as shown in Fig.2.

3.1. Standard Target

Let us at first theoretically investigate the acceleration of ST by PARCIPHAL changing laser intensity I from 10^6 to 10^{11} (MW/m^2) for an aluminum target placed in atmospheric pressure of 0.01atm. Laser pulse τ is 5ns and wavelength is 1064 nm. Figure 3 shows the time evolution of ablation process for various laser intensities. High temperature region can be seen not on the surface of target but in the gas neighbor to the surface as shown by the arrows. This is because plasma that absorbs laser energy is generated by ablation. Plasma temperature becomes a few tens of eV. After 10ns, high density of 0.1kg/m^3 region appears at the head of ablation. It is the blast wave through ambient gas generated by so-called LSD (Laser-Supported Detonation) shock wave, whose pressure and temperature are also higher than those in the other region.

In the simulation of the standard target (ST) (the single-layer target), C_m has the (maximum of 17 [N·sec/MJ] at 7×10^3 MW sec$^{1/2}$/m^2 (1×10^8MW/m^2) as shown in Fig.4 because laser energy is too small to drive the aluminum target when I is less than the optimal intensity. In ST's, most of the energy is transferred to low density gas and only a small fraction of energy (normally less than a few percent) is used to drive a target. On the other hand, when I is larger, laser-produced plasma absorbs most of the laser energy by inverse Bremsstrahlung and shields the target surface. This is justified by viewing temperature profile in Fig.3. Actually, plasma temperature reaches a few hundreds eV because most of laser energy is absorbed by plasma for 10^9W/m^2.

3.2. Exotic target

Next, we investigate layered pendulum that consists of aluminum target over-coated with transparent material. The layered target, which we call "exotic target (ET)" hereafter relies on the enhanced coupling efficiency of the target geometry in which a transparent material overlies a metal layer. In order to investigate this coupling, we did a systematic survey with experiments and simulations.

Figure 4 includes the experimental results by the LHMEL Nd:glass laser at Wright-Patterson AFB, Ohio.[10] The laser consists of four 64-mm diameter flashlamp-pumped glass rods fed by two separate oscillators which were combined on a polarization beam splitter at their input aperture. Mutual isolation of the oscillators was accomplished with a Faraday rotator for one and a polarizer- $\lambda/4$ plate unit for the other. Relative timing of the two oscillators could be adjusted from 0-100μs with 1μs jitter. The purpose of this arrangement was to test the effect of double pulses on coupling which will not be discussed here. In this experiment, glass is used as a tamper. The laser parameters are given in Table.1.

The corresponding simulation with PARCIPHAL is also depicted in Fig.4 and agrees well with experimental ones showing its reliability and hence we expect larger coupling coefficient for lower laser intensity beyond the experimental data. In contrast to the ST, C_m of the ET increases even with decreasing intensity I because the space between the two layers is filled with evaporated gas , providing a large amount of energy to drive the metal target, while the reduced C_m at high laser intensity is the same as the case of ST, i.e., it is dominated by plasma shielding.

Intense plasma formation has two independent effects in the present situation. First, it limits the laser energy which can reach the ablator surface above a well-defined threshold. Figueira, et al.[14] show with experimental examples how laser-produced plasma transmission self-adjusts to limit the transmitted energy to a fixed value above the threshold for this "clamping" behavior. Second, it forces an increasing fraction of the incident laser energy to be converted to high-velocity plasma kinetic energy, degrading the momentum coupling efficiency. This degradation occurs because the definition of C_m (momentum/energy $\sim 1/v$) causes it to be small for high ejecta velocity.

3.3. Liquid Tamper vs Solid Tamper

Similar experiments have been performed also for water overlay. Figure 5(d) shows the systematic increase of C_m we observed for water overlay compared with acrylic overlay. In the case of water, both pendulum and load cell measurements are compared for the calibration of the load cell. In order to examine this increase, we have performed a simulation with 0.1mm thick overlay for a 2.01×10^4 MW.sec$^{1/2}$/m^2 laser beam. As Fig.5(a) shows, the acrylic overlay did not burn through because of material strength and all the layer even outside the laser spot moves together. This is actually observed in the experiments and we are able to retrieve the acryl of complete shape as it was. In contrast, only a part of the layer (corresponding to the laser spot size) is exploded in the water overlay [see Fig.5(b)]. As shown in Fig.5(c), C_m of water gradually increases in time. Since it needs huge computation time to simulate the overlay of mm size, we simulated 0.1mm thickness and C_m was consequently lower than experiments.

We must remember that the data of glass shown in Fig.4 and Fig.5(d) are taken in vacuum condition while others are in atmospheric pressure. Our experimental results show an increase of C_m in standard target with increasing atmospheric pressure and this is because air acts like a second tamping layer. However, the back-pressure dependence with the exotic target may be smaller because of the large tamping effect that is already included as overlay.

4. MICRO-AIRPLANE

Since the performance of ET target revealed the promising results, we shall turn to practical application of this concept. As an important near-future application, we propose a propulsion concept in which a laser drives a micro-airplane that can be used for observation of climate and volcanic eruption, and demonstrate it by experiments with a 590mJ/5ns YAG laser. The micro-airplane can be less than 100g sufficient for loading observation and communication devices like cell phone if no engine and controlling devices are necessary. Since the vertical launch of the rocket of around 100g has already been demonstrated,[3] micro airplane is much easier and does not need larger laser energy because it can fly with wing and need not be launched vertically.

4.1. Flying Micro-airplane

Two types of paper airplane are examined with two different ablation structures. In one type, a 38mm×30mm×5mm airplane of 0.1g-weight is placed on the platform with a guiding groove and is irradiated by one pulse of YAG laser. Figure 6 shows the most frequently observed behavior, in which the airplane makes a circular flight and turns back. The ablation structure is a 3.5mm×3.5mm×0.1mm-thick aluminum foil over-coated with 0.6mm-thick acryl. Figure 7 shows the second type of airplane of 39mm×56mm×15mm size and 0.2g-weight. In this case, the laser target is a 3mm-diameter, 0.014g water droplet attached to the aluminum foil. In both figures, large bright spot on the left shows the laser irradiation zone.

The measured velocity of the airplane for the case in which the flight path was normal to the camera was 1.4m/sec at the beginning. This gives C_m =237N·sec/MJ , in rough agreement with the scaling law in Fig.4 for = 1.8×10^4 MW.sec$^{1/2}$/m^2 based on the 760μm focal spot diameter. Following this scaling law, we already achieved 5000N·sec/MJ with a larger laser on an ET target, and much larger efficiency of $\sim 10^5$N·sec/MJ is expected from simulation results. Therefore the use of exotic target concept for a propulsion system is attractive for practical applications.

4.2. Water Supply for Repetitive Propulsion

For practical application, the overlay structure must be repetitively constructed. Phipps et.al.[15] proposed the use of rolling film like video tape. In the present case, however, we prefer to use water overlay because of several advantages : (1) higher efficiency (2) easier arrangement (3) automaic collection from air and so on. For water supply, we here propose a structure shown in Fig.8, where water is contained in a narrow space between two plates with a small hole of 2mm in one side. We have demonstrated that the water did not escape from the hole due to surface tension and was quickly supplied after irradiation as shown in Fig.9.

Let us estimate the recovering time of water surface. The effect of surface tension is given as follows.

$$M\frac{dV}{dt} = \frac{\sigma S}{R} \tag{6}$$

where $M = 4\pi R^3\rho/3$ is the mass of water droplet of radius R and S the surface area. Thus the time scale of restoration is

$$t = \left(\frac{\rho R^3}{3\sigma}\right)^{1/2}. \tag{7}$$

Therefore if the required repetition time should be less than a second, the radius of water must be less than $(3\sigma/\rho)^{1/3}$ which is 6cm and 2mm size of hole is sufficient for the recovery within a second. In turn, if the hole size is 2mm, the restoration time by surface tension is 0.006 sec and we can use the overlay structure in such a short time cycle without any mechanism to drive the structure.

Water has another advantage since it is included in the air and can be continuously collected by condensation from the air.

5. FUTURE

The result in Fig.4 is very exciting. The maximum value $\sim 10^5$ N.sec/MJ obtained by simulations means that one pulse of 1MJ laser can give a velocity 10m/sec to an airplane of 10tons. After 30 pulses it gains the speed of sound !!! Thus much smaller laser is sufficient for practical applications. Even 1MJ laser is not a dream but Lawrence Livermore National Laboratory is building it for the purpose of laser-driven fusion. Although the repetition rate is an order of day at present, 1Hz operation will be possible near future. Not only such airplane but we can drive ships skimming on the water surface. Needless to say, the space rocket in outer space can also be driven. In the last case, however, we need to find water in outer space from the object like comet.

Tracing the airplane is another difficult subject. NASDA (National Space Development Agency of Japan) is testing acquisition and tracking technology for laser inter-satellite communications(see Fig.10). This technology can be used for airplane.

If we can use the phase-conjugation mirror in lasers and array of prisms at the airplane, we can scan over the neighboring area of airplane by small signal laser and only signal that will return back from prisms is amplified by the amplifier with phase-conjugation mirror and is directed back to the airplane again. With the speed of light, the propagation time of light in the distance of 1km

is 3μsec and airplane of 300m/sec moves only 1mm during this period. In such a system, the water supply is composed of many holes like lotus nut not like a single hole in Fig.8 and the exact location of hole is not necessarily illuminated.

We should notice that control of the airplane can also be accomplished by direct ablation of wing material, or heating of shape memory alloy on the wing which can be deformed by laser heat deposition without ablation. The paper by K.Aoki *et.al.* in the same proceedings reports the electrical output from solar panel heated by laser and its use for the movement of shape memory alloy.

This kind of technique is not only limited to flying objects but can be applied to other area as follows.

- **Micro-ship in Inner Space** We can drive a micro-ship or micro-capsule of medicine by a X-ray laser whose wavelength is 40 A. Because 80% of human body is composed of water and human body is transparent to this so-called "water-window" X-ray, the laser will be able to shine the micro-ship from outside (see Fig.11). The ship can have a structure as shown in Fig.11(Left) and is equipped with focusing lens made by Fresnel zone plate because it may be difficult to focus the laser into a small size. By this method, X-ray need not be focused onto the micro-ship and low intensity of unfocused X-ray may not cause serious damage to the human body. One of the authors (K.Yoshida) already developped a microscopic Fresnel zone plate which is 47μm size and succeeded to focus 1.45A X-ray into 0.5μm spot.[16] If we need the laser intensity of $I\tau^{1/2} = 10\text{MW}\cdot\text{sec}^{1/2}/\text{m}^2$ for ablation as in Fig.4, the laser power and energy delivered to this spot size are 28mW and 142pJ for 5ns pulse. In order to demonstrate the underwater acceleration of the ship, we illuminate the aluminum pendulum of 7mm×5mm×1.5mm size contained in a glass of water. Figure 15 shows the time sequence of the movement. The focal spot size was 900 μm. The estimated C_m of underwater acceleration is 137 N·sec/MJ for 300mJ and 212 N·sec/MJ for 560mJ lasers, while in the air it is 39 N·sec/MJ for 300mJ and 61 N·sec/MJ for 560mJ lasers. Although the pendulum should hardly move owing to a large drag inside water, the momentum gained by the pendulum in the water is three times larger than that in the air. This is due to the efficiency enhancement by water overlay.

- **Micro-Robot in Nuclear Reactor Accident** At the accident of nuclear power reactor, a lot of neutron will be emitted and make electronic devices useless. If we need to send robots to this place, the robots must be driven by some means. We are planning to drive these robots by laser in a long distance. We can use shape memory alloy heated by laser to make movement of robots as well as direct ablation process. These robots will be carried by the ship given below.

- **Mini-Airship** In Japan, we have a project for making airship for telecommunication with cell phone (see Fig.12). Usually the satellite is used but it is too expensive. For this purpose, we can cover the Japan island by several airships. We are planning to use the laser drive for controlling and movement. The small size of airship can carry the micro-robot given above.

- **Kite Plane** With the collaboration with National Institute for Environmental Studies, we are planning to drive a kite-plane(see Fig.13) for atmospheric obeservation and so on. Micro-scopic kite plane or feather plane can fly inside the lungs in human body also driven by X-ray lasers.

Most of the subjects will be turned into reality within few decades. Aiming at these goals, we have just started the collaboration program (Fig.14), which is not yet supported as the National project but is now under progress with their own budget. The goal of each group is

- **(1) Tokyo Institute of Technology** Demonstration of 100g micro-airplane by 100J laser. Development of micro-ship and X-ray laser. Development of controlling and tracking devices.

- **(2) Photonic Associates, USA** Planning and discussion.

- **(3) Osaka Institute of Technology** Making new laser of sub Hz at more than 5J based on diode array.

- **(4) Japan Atomic Energy Research Institute** Development of airship and its control and driving by laser.

- **(5) National Institute for Environmental Studies** Development of micro-airplane for atmospheric observation (kite-plane).

- **(6) National Institute of Advanced Industrial Science and Technology** Development of robot carrier and micro-robot driven by laser without electronic devices.

Acknowledgement

This work was carried out under the collaborating research program at the National Institute for Fusion Science of Japan.

REFERENCES

1. A. Kantrowitz, "Propulsion to Orbit by Ground-Based Laser," *Astronaut. Aeronaut.* **10**, pp. 74 ,1972.
2. C. R. Phipps,Jr. *et.al.*, "Impulse coupling to targets in vacuum by KrF,HF,and CO_2 single-pulse lasers," *J.Appl.Phys.* **64**, pp.1083–1096, 1988.
3. L. N. Myrabo and F. B. Mead, Jr., "Ground and Flight Tests of a Laser Propelled Vehicle ," AIAA98-1001, Aerospace Sciences Meeting & Exhibit,36th, Jan12-15,1998
4. C. R. Phipps and M. M. Michaelis, "LISP:Laser impulse space populsion," *Laser and Particle Beams* **12** , pp.23–54, 1994.
5. N. C. Anderholm, "Laser-Generated Stress Waves," *Appl.Phys.Lett.* **16**, pp.113–115 , 1970.
6. F. Winterberg, "Recoil Free Implosion of Large-Aspect Ratio Thermonuclear Microexplosion," *Lettere al Nuovo Cimento* **16**, pp.216–218 , 1976.
7. H. Azechi, N. Miyanaga, S. Sakabe, T. Yamanaka and C. Yamanaka, "Model for Cannonball-Like Acceleration of Laser-Irradiated Targets," *Jpn.J.Appl.Phys.* **20**, pp.L477–L480, 1981.
8. T. Yabe and K. Niu, "Numerical Analysis on Implosion of Laser-Driven Target Plasma," *J.Phys.Soc.Japan* **40** , pp.863–868 , 1976.
9. R. Fabbro, J. Fournier, P. Ballard, D. Devaux and J. Virmont, "Physical Study of Laser-Produced Plasma in Confined Geometry," *J.Appl.Phys.* **68**, pp.775–784 , 1990.
10. C. R. Phipps, D. B. Seibert II, R. Royse, G. King and J. W. Campbell,"Very High Coupling Coefficients at Low Laser Fluence with a Structured Traget," III International Symbosium on High Power Laser Ablation, Santa Fe, 2000, SPIE Vol.**4065** pp.931–937.
11. A. Sakurai,"Blast Wave from a Plane Source at an Interface," *J.Phys.Soc.Japan* **36**, pp.610–610, 1974.
12. see for review of the method T. Yabe, F. Xiao and T. Utsumi, "Constrained Interpolation Profile Method for Multiphase Analysis," *J. Comput. Phys.* **169**, pp.556–593 , 2001.
13. T. Yabe, "A Universal Numerical Solver for Solid, Liquid and Gas - Application to Laser-Induced Melting and Evaporation -," SPIE Proc. *On Laser-Assisted Microtechnology* Vol.**4157** pp.1–7 ,2000.
14. J. F. Figueira, S. J. Czuchlewski, C. R. Phipps, Jr., and S. J. Thomas, "Plasma-breakdown retropulse isolators for the infrared," *Appl. Opt.* **20**, pp.838–841, 1980.
15. C. Phipps and J. Luke,"Diode Laser-Driven Microthrusters : A New Departure for Micropropulsion," *AIAA Journal* **40**, pp.310-318, 2002.
16. S. Tamura, K. Ohtani, N. Kamijyo, K. Mori, T. Maruhashi, K. Yoshida, Y. Suzuki and H. Kihara,"Fabrication and Testing of Cu-Al Multi-Layer Fresnel Zone Plate," *Shinkuu(Vaccuum)* **40**, pp.234–237, 1977 (in Japanese).

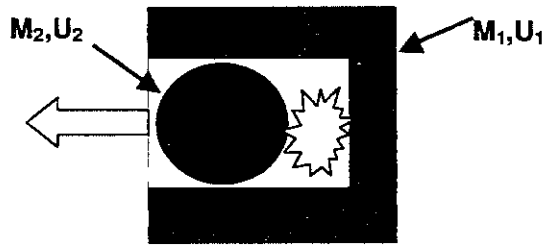

Figure 1. Cannnon ball M_2 is effectively driven by large tamper M_1.

Figure 2. (Left) Structure of Standard target (ST) and (Right) Exotic target(ET).

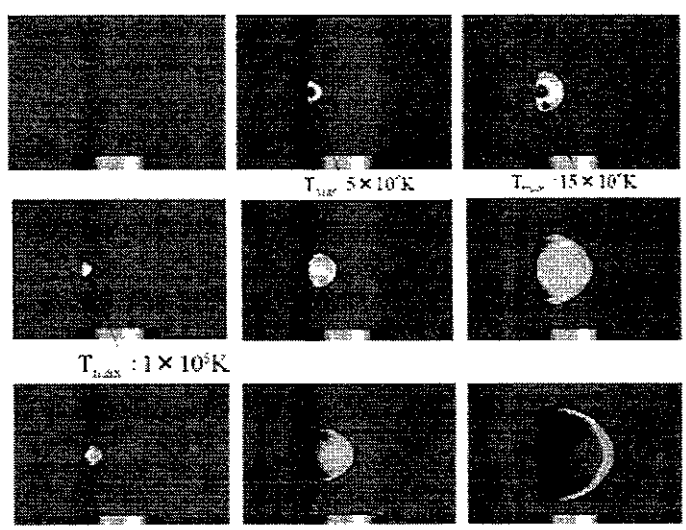

Figure 3. Simulation results of ablation. Time is 6, 10, 14ns from the top to the bottom. Laser intensities are $10^7, 10^8, 10^9$ MW/m^2 from left to right.

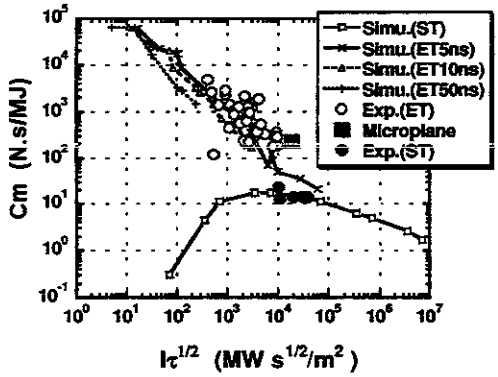

Figure 4. Dependence of C_m on $I\tau^{1/2}$. The open circles show experimental results using the LHMEL Nd.glass laser and the closed squares represent the result of the micro-airplane in section 4. In the simulation, the pulse width of the laser was changed from 5ns to 50ns.

Table 1. LHMEL Laser Parameters

Parameter	Osc.1	Osc.2
Energy	40J‡	30J
Pulsewidth	25ns	50-100ns
Total*	70 J	
Target intensity**	1.3 GW/cm^2	
Repetition rate	1/10minutes	

‡ Amplifier output with this oscillator
. . Varied 3 –70J via flashlamp energy & number
**At focus of a 1-m FL mirror in target chamber

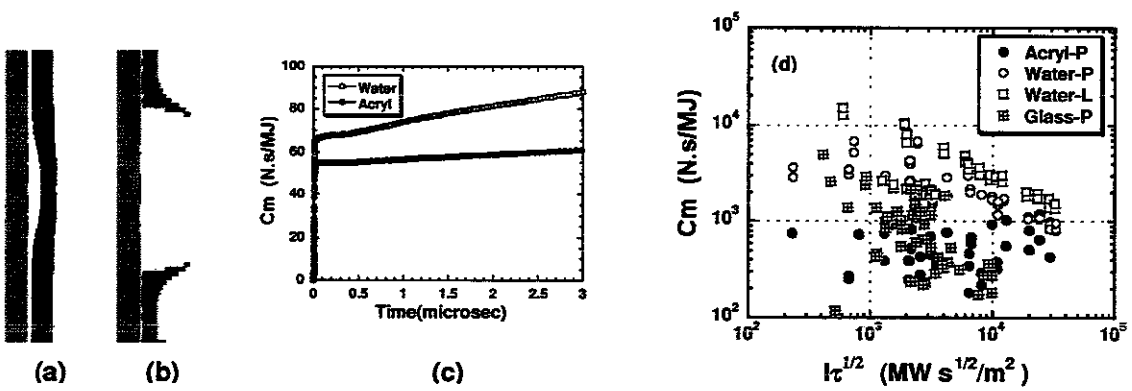

Figure 5. Density contour by simulation at 3×10^{-6} sec for (a) acrylic overlay and (b) water overlay. (c) Time history of C_m. (d) C_m for water, acrylic, glass overlays. Data of glass overlay are the same as Fig.4 and experimental condition is different from acryl and water. Water-P and Water-L stand for water overlay measured by pendulum and load cell.

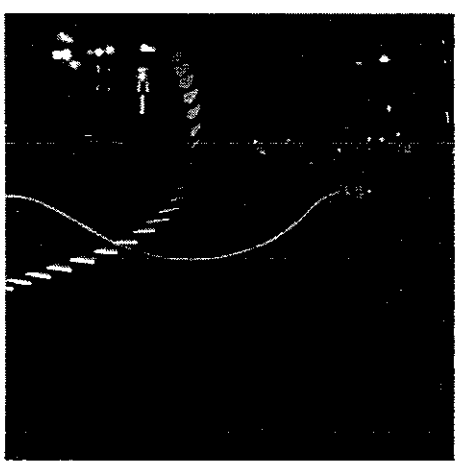

Figure 6. The flight trajectories of a micro-airplane with acryl overlay.

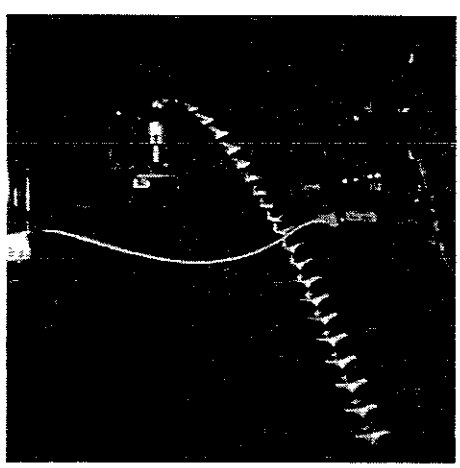

Figure 7. The flight trajectories of a micro-airplane with water droplet overlay.

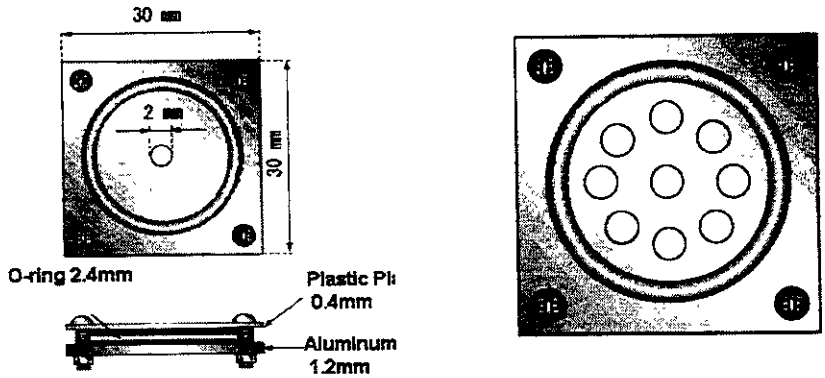

Figure 8. Water supply system for repetitive propulsion.(Left) Single hole used in the experiments. (Right) Multi-holes like lotus nuts.

Figure 9. Demonstration of water supply system. (a) before irradiation, (b) irradiation, (c) after irradiation.

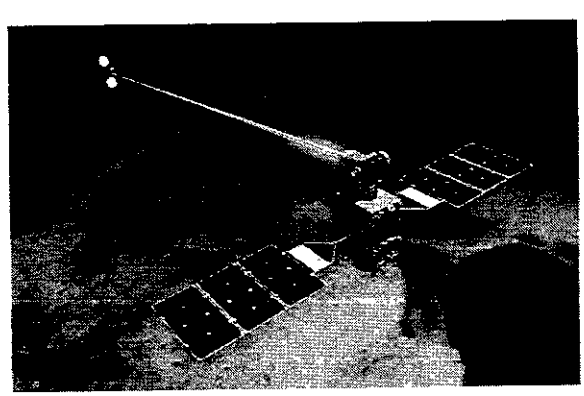

Figure 10. Optical Inter-Orbit Communications Engineering Test Satellite - OICETS aims to demonstrate pointing, acquistion and tracking technology(Courtesy of NASDA).

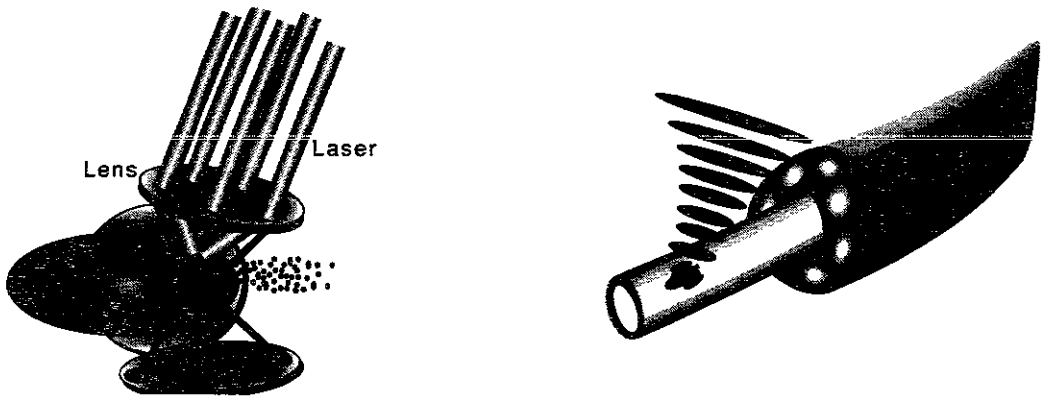

Figure 11. (Left) The microship is equipped with several Fresnel zone plates and then X-ray needs not be focused onto the ship. This is important to avoid un-necessary damage to the body.(Right) The microship can go along the blood or lymphatic vessel driven by "water-window" X-ray laser placed outside of human body.

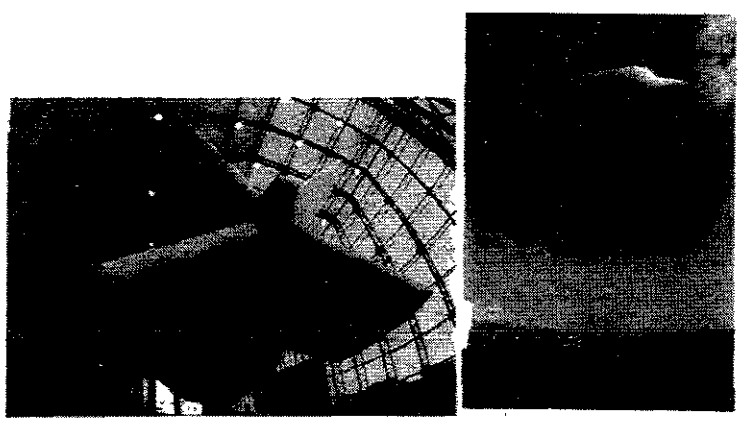

Figure 12. The airship constructed at Japan Atomic Energy Research Institute in colaboratin with National Institute of Advanced Industrial Science and Technology aimed at electro-telecommunication. The laser can also be used to drive and control this ship as well as a small-size airship for carrying micro-robot.

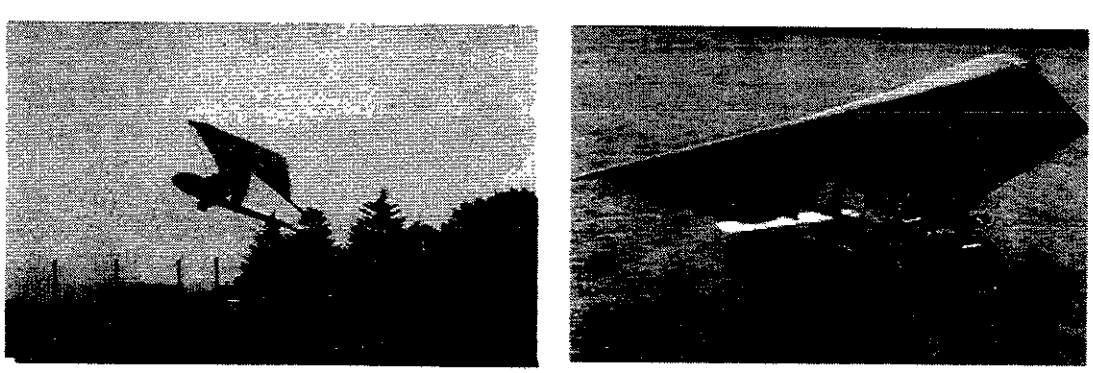

Figure 13. A kite plane developped at National Institute for Environmental Studies. This plane is at present driven by propeller and controlled by radio frequency wave. It somtimes looses the control and cannot fly at high altitude because the propeller does not work at such altitude. Laser drive is expected to improve this situation.

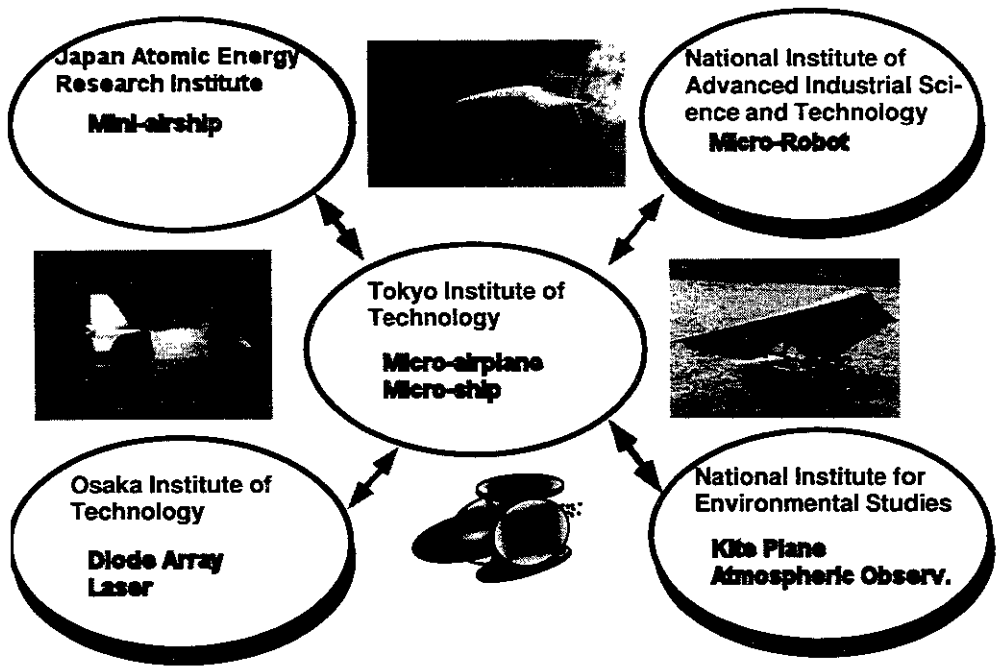

Figure 14. Collaboration program for various laser-driven vehicles.

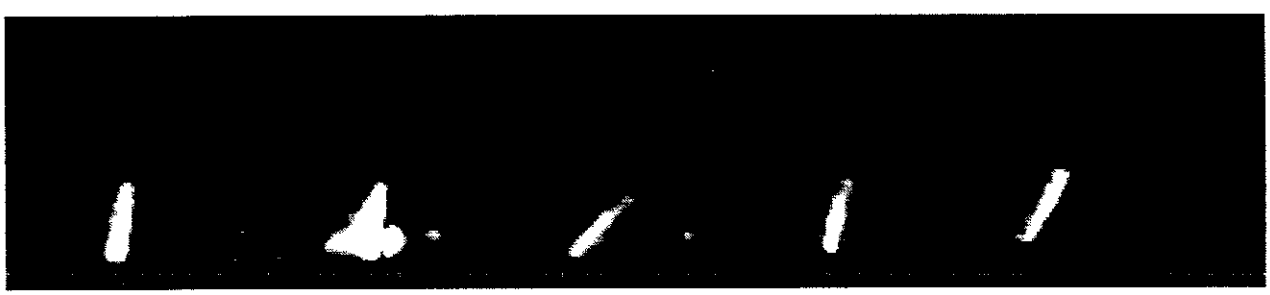

Figure 15. Pendulum driven by 300mJ laser inside water.

NIFS-713 Y Matsumoto, S.-I Orkawa and T Watanabe
Field Line and Particle Orbit Analysis in the Periphery of the Large Helical Device
Sep. 2001

NIFS-714 S. Toda, M Kawasaki, N Kasuya, K Itoh, Y Takase, A. Furuya, M Yagi and S -I Itoh
Contributions to the 8th IAEA Technical Committee Meeting on H-Mode Physics and Transport Barriers (5-7 September 2001, Toki, Japan)
Oct. 2001

NIFS-715 A. Maluckov, N Nakajima, M Okamoto, S Murakami and R. Kanno
Statistical Properties of the Particle Radial Diffusion in a Radially Bounded Irregular Magnetic Field
Oct. 2001

NIFS-716 Boris V. Kuteev
Kinetic Depletion Model for Pellet Ablation
Nov. 2001

NIFS-717 Boris V. Kuteev and Lev D Tsendin
Analytical Model of Neutral Gas Shielding for Hydrogen Pellet Ablation
Nov. 2001

NIFS-718 Boris V. Kuteev
Interaction of Cover and Target with Xenon Gas in the IFE-Reaction Chamber
Nov. 2001

NIFS-719 A Yoshizawa, N Yokoi, S.-I Itoh and K Itoh
Mean-Field Theory and Self-Consistent Dynamo Modeling
Dec. 2001

NIFS-720 V.N. Tsytovich and K. Watanabe
Universal Instability of Dust Ion-Sound Waves and Dust-Acoustic Waves
Jan 2002

NIFS-721 V.N. Tsytovich
Collective Plasma Corrections to Thermonuclear Reactions Rates in Dense Plasmas
Jan. 2002

NIFS-722 S. Toda and K Itoh
Phase Diagram of Structure of Radial Electric Field in Helical Plasmas
Jan. 2002

NIFS-723 V.D. Pustovitov
Ideal and Conventional Feedback Systems for RWM Suppression
Jan. 2002

NIFS-724 T. Watanabe and H. Hojo
The Marginally Stable Pressure Profile and a Possibility toward High Beta Plasma Confinement in LHD
Feb. 2002

NIFS-725 S.-I. Itoh, K. Itoh, M. Yagi, M. Kawasaki and A. Kitazawa
Transition in Multiple-scale lengths Turbulence in Plasmas
Feb. 2002

NIFS-726 S.-I. Itoh, A. Kitazawa, M Yagi and K. Itoh
Bifurcation and Phase Diagram of Turbulence Constituted from Three Different Scale-length Modes
Apr. 2002

NIFS-727 M. Nagata
Preliminary Experiment on the Negative Magneto-Resistance Effect in a Weakly Ionized Discharge Plasma
Apr. 2002

NIFS-728 K. Akaishi and M. Nakasuga
Calculation of Hydrogen Outgassing Rate of LHD by Recombination Limited Model
Apr. 2002

NIFS-729 Y. Kondoh, T. Takahashi and J. W. Van Dam
Proof of Non-invariance of Magnetic Helicity in Ideal Plasmas and a General Theory of Self-organization for Open and Dissipative Dynamical Systems
Apr. 2002

NIFS-730 S.-I. Itoh and K. Itoh
From Dressed Particle to Dressed Mode in Plasmas
May 2002

NIFS-731 R. Kanno, N. Nakajima and H. Takamaru
Path Integral Approach for Electron Transport in Disturbed Magnetic Field Lines
May 2002

NIFS-732 H. Sugama and S Nishimura
How to Calculate the Neoclassical Viscosity, Diffusion, and Current Coefficients in General Toroidal Plasmas
May 2002

NIFS-733 S. Satake, M. Okamoto and H. Sugama
Lagrangian Neoclassical Transport Theory Applied to the Region near the Magnetic Axis
June 2002

NIFS-734 S. Murakami, A Wakasa, H. Maaβberg, C.D. Beidler, H Yamada, K.Y. Watanabe and LHD Experimental Group
Neoclassical Transport Optimization of LHD
June 2002

NIFS-735 T. Yabe, C Phipps, K. Aoki, M. Yamaguchi, Y Ogata, M Shiho, G. Inoue, M. Onda K Horioka, I Kajiwara, S Maehara and K. Yoshida
Laser-Driven Vehicles - from Inner-Space to Outer-Space -
June 2002